Asian Journal of Chemistry; Vol. 29, No. 9 (2017), 1953-1958

ASIAN JOURNAL OF CHEMISTRY

https://doi.org/10.14233/ajchem.2017.20646

Exploring Viscoelastic Characteristics of Polymer-Water Solutions by Viscometric Analysis

SHITANSHU DEVRANI, RAJAT SHARMA, M.P. RAJESH and ASHISH KAPOOR*

Department of Chemical Engineering, SRM University, Kattankulathur-603 203, India

*Corresponding author: E-mail: ashishkapoorsrm@gmail.com

Received: 13 March 2017; *Accepted*: 13 May 2017; *Published online*: 15 July 2017; AJC-18472

Addition of small concentrations of certain high molecular weight polymers to flowing fluids can drastically reduce the turbulent friction. The mechanism is caused by the interaction of the elongated polymer molecule chains and the solvent molecules. The elongated structure of polymer acts as an eddy stress absorber and in turns ensures overall drag reduction between fluid layers. This can also be stated as the development of viscoelastic nature in the subject fluid. The present study compares the effects of the addition of two polymers namely polyacrylamide (PAM) and polyethylene oxide (PEO) in water, a Newtonian fluid. An experimental study using a viscometer is analyzed to showcase the viscoelastic nature developed by water on addition of polymers over a range of ppm concentrations. The results are in agreement with data reported in literature that viscoelastic nature is triggered on addition of these polymers.

Keywords: Viscoelasticity, Drag reduction, Eddy viscosity, Polymer additives, Polyacrylamide, Polyethylene oxide.

INTRODUCTION

A remarkable reduction in energy losses in turbulent flows can be attained by the addition of minute amounts of certain polymers in water or in organic solvents. This rheological drag reduction phenomenon using polymer additives was firstly reported in the late 1940s [1]. Since then it has found several practically useful applications, including flow in pipelines, heating and cooling systems, sewer systems and locomotion of ships and underwater vehicles [1,2].

The drag reduction effect is due to the ability of the polymer to sustain large elongation by developing an elastic nature. It leads to stabilization of the turbulent boundary layer, resulting in less turbulent energy generation and hence reduced dissipation. Drag-reducing polymer solutions exhibit visco-elastic fluid like behaviour. A notable feature of the viscoelastic polymer solution is that stress does not instantaneously reduce to zero on stopping the fluid motion. Rather, it decays with some characteristic time that is typically of the order of seconds to few minutes [2]. The frictional drag reduction by polymer additives in a confined flow is commonly attributed to be an outcome of the interaction between viscoelasticity and turbulence in the fluid flow. Even though the polymers are mainly active on the smallest length scales, still they have capability of influencing macroscale flows by which the drag is determined [1].

Any fluid flow is broadly classified into two kinds, turbulent flow and laminar flow. The high Reynolds number conditions during turbulent flow lead to the formation of eddies [3-5]. During industrial transportation of fluids, typically high Reynolds numbers are reached which trigger the formation of eddies in the flow regime. These eddies are circular whirlpools formed because of the vacuum created due to sudden pressure drop at very high velocities obtained at high Reynolds numbers. The resulting phenomenon of drag is characterized by the term eddy viscosity [6,7]. In the study of turbulence in fluids, a common practical strategy for calculation of turbulence is to ignore the small scale vortices in the motion and to estimate the large-scale flow phenomenon with an eddy viscosity that captures the characteristics of transport and dissipation of energy in the small-scale flow. In the case of higher Reynolds numbers such type of eddy viscosities cause a significant rise in pumping costs [8].

The objective of this study is to investigate the effect of addition of polymers to Newtonian fluids and draw an inference over the drag reduction phenomenon caused by these polymers in fluid flow. It is believed that the research findings can assist in design and development of fluid-flow related systems, including piping design in which polymer drag reduction can be exploited in a cost-effective way.

Mathematical model: The mathematical model equation employed here to understand polymer solution behaviour in viscometer is a simplified form of Navier-Stokes equation for flow in a cylindrical pipe and is adapted from the general equations developed in the work of [1]. Addition of polymer to fluid introduces a new term in the overall mathematical

model of fluid flow designated as the polymeric component. The model is given as:

$$-\frac{r}{2}\left(\frac{dP}{dz}\right)=\rho\left\langle u_z' u_r'\right\rangle-\mu\left(\frac{dU_z}{dr}\right)-\gamma_{P,r} \quad (1)$$

where P is the pressure exerted by the model fluid, r is the radial distance in the model pipe, z is the axial distance in the model pipe, ρ is the density of fluid, μ is the viscosity of fluid, U_z is the velocity of fluid in axial direction, u_z' is the fluctuant velocity in axial direction, u_r' is the fluctuant velocity in radial direction and $\gamma_{P,r}$ is the counter recoil force due to the nature of polymer fluid. The axial and radial directions are denoted by subscripts z and r respectively.

The model equation is essentially a force balance during turbulent conditions on a microscopic scale for a fluid mixed with a drag reducing polymer. Left hand side (LHS) expression in eqn. 1 originates from the force exerted on a molecule at the centre of the pipe flowing in z-direction. Right hand side (RHS) expression originates from the total mean shear stress consisting of turbulent, laminar (or viscous) and polymeric components, respectively as indicated in eqn. 1. The turbulent component is the first term on right hand side expression and is determined by Reynolds stress tensor in axial and radial directions of fluid flow. The second term designates the viscous component with the negative sign implying that the force acts in opposite direction to that of the fluid flow. The last term indicates the polymeric component, which is the contribution factor of the long chain polymers in the overall stress on the fluid.

The turbulent shear stress has been shown to be suppressed by the polymer additives [2,9,10]. This implies a decreased correlation between the stream wise and the normal velocity fluctuations. The resulting phenomenon is known as Reynolds stress deficit. In this phenomenon, the turbulent shear stress and the viscous shear stress do not add up to give the linear variation of the total shear stress over the pipe or channel cross section, *i.e.* the term $\gamma_{P,r}$ is significant. The mathematical model ensures no backtracking of molecules to cause vortex formation. These eddies are the essential source of resistance to motion causing eddy viscosity at high Reynolds numbers. This implies that the long chain polymers cause a definite recoil mechanism which results in the significant reduction in pressure drop across a channel during turbulent flows [8,11-15]. The mechanism points towards a shear thinning or viscoelastic nature of the fluid, which is triggered by the addition of the long chain polymers.

EXPERIMENTAL

Experiments were conducted using two polymers, namely polyacrylamide (PAM) (anionic, 16 % hydrolyzed) of molecular weight 20×10^6 g/mol (Merck) and polyethylene oxide (PEO) of molecular weight of 6×10^6 g/mol (Merck). The structural formula of the polymers is shown in Fig. 1. Distilled water served as the model Newtonian fluid.

Experimental set up and procedure: Brookfield rotational viscometer (Brookfield Engineering, USA) used in this work is a typical on-line instrument that fulfils the criteria of 4 Rs, *i.e.*, representative sampling, relatability, reliability and

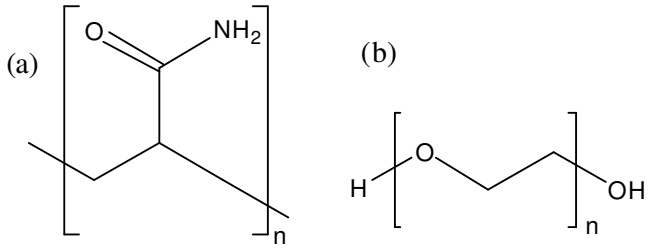

Fig. 1. Chemical structure of (a) polyacrylamide (PAM) and (b) polyethylene oxide (PEO)

robustness of the operation [3]. The instrument consists of a concentric cylindrical arrangement that can operate in- or on-line. It has an open-ended variant that can be mounted into the wall of a vessel container [7,16-19]. Spindle is mounted in a chamber through which the liquid of interest flows, the schematic arrangement is shown in Fig. 2. The speed of the motor driving the outer cylinder can be varied or fixed and the torque produced on the inner cylinder causes a small twist of the sealed torque-tube supporting it. The twist is transmitted through the wall without friction and is measured on a rotation transducer mounted outside the chamber.

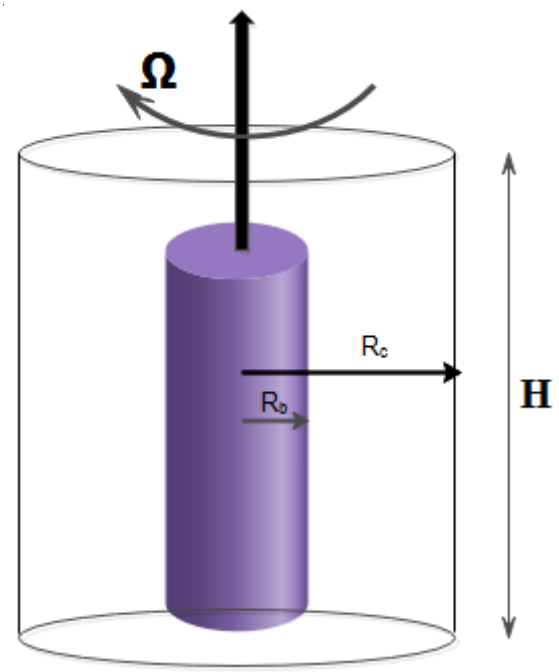

Fig. 2. Schematic representation of spindle arrangement in viscometer

The shear rate can be set to any value between about 1 and 1000 s^{-1} and is a combination of the effect of the motor speed and the gap between the cylinders. The principle operation of this instrument is to drive a spindle, which is immersed in the test fluid through a calibrated spring. The viscous drag of the fluid against the spindle is measured by the spring deflection. Spring deflection is measured with a rotary transducer. The system provides continuous sensing and display of the measurement during the entire test [3,8,17]. The measurement range of viscosity (in centiPoise or milli Pascal-seconds) is determined by the rotational speed of the spindle, the size and shape of the spindle, the container the spindle is rotating in and the full scale torque of the calibrated spring [3].

$$\text{Viscosity } \mu = (\text{Shear stress/Shear strain rate}) \quad (2)$$

where viscosity is in Poise, shear stress in dyne/cm^2 and the rate of shear in s^{-1}. The full scale torque of viscometer used in this work is 673.7 dyne/cm^2 and torque is linear with the scale reading. A material requiring a shear stress of 1 dyne/cm^2 to produce a unit shear rate of 1 s^{-1} has a viscosity of 1 Poise (100 cP). The rotational viscometer employs the following equations to determine shear strain rate and shear stress.

$$\text{Shear strain rate } \frac{d\gamma}{dt} = \left(\frac{2\Omega R_c^2 R_b^2}{x^2 (R_c^2 - R_b^2)} \right) \quad (3)$$

$$\text{Shear stress } \tau = \frac{M}{2\pi R_b^2 L} \quad (4)$$

where μ is the viscosity of fluid, τ is the applied stress, M is the torque input by instrument, L is the effective length of spindle, R_c is the radius of container, R_b is the radius of spindle, x is the radius at which shear rate is measured and Ω is the angular velocity of spindle. Shear strain rate is often abbreviated as shear rate or strain rate.

The aforementioned equations are used to calculate the corresponding strain rates for the torques applied at measurement radius x = 1 cm. A similar approach could be used to find strain rates at any distance from the spindle surface inside the hollow cylinder. Different sample solutions of polyacrylamide and polyethylene oxide in water of concentrations ranging from 0 to 600 ppm are prepared, with 0 ppm solution being pure distilled water. Each solution is prepared carefully by adding the pre-calculated amount of polymer into 100 mL of distilled water. Spindle (size no.18) is inserted into the hollow cylinder containing the sample solution. The viscometer-user interface has an adjustable display for rotational speed (rpm), viscosity (cP), torque delivery (or applied) (% dyne) and temperature (°C). The rotational speed is adjusted to values ranging from 30 to 200 rpm and corresponding values of torque delivery %, viscosity and temperature are recorded. The experimental data is collected for rotational speeds of 30, 50, 70, 100, 120, 130, 150, 170 and 200 rpm.

RESULTS AND DISCUSSION

Variation of torque against rotational speed: The variation of applied torque to the spindle against spindle speed for the subject fluids polyacrylamide and polyethylene oxide solutions in water is plotted in Figs. 3 and 4 respectively. The comparison of values for pure water case (0 ppm) with polymer added aqueous solutions points out that the applied torque by the spindle increases with rotational speed for all the cases. However, for 100, 200 and 300 ppm polyethylene oxide solutions there is an initial decrease followed by a steep rise in torque with rotational speed. This is a consequence of the fact that in order to increase the rotation of the spindle the viscometer shaft has to be applied with the greater torque.

For polyacrylamide (Fig. 3), addition of polymer from 70 to 600 ppm gives great variation on the applied torque. The closest proximity to water is achieved for 70 ppm. The difference in the range of torque applied is close to water at low rotational speeds but only increases with the increase in rotational speeds. The applied torque values for 70 to 500 ppm solutions

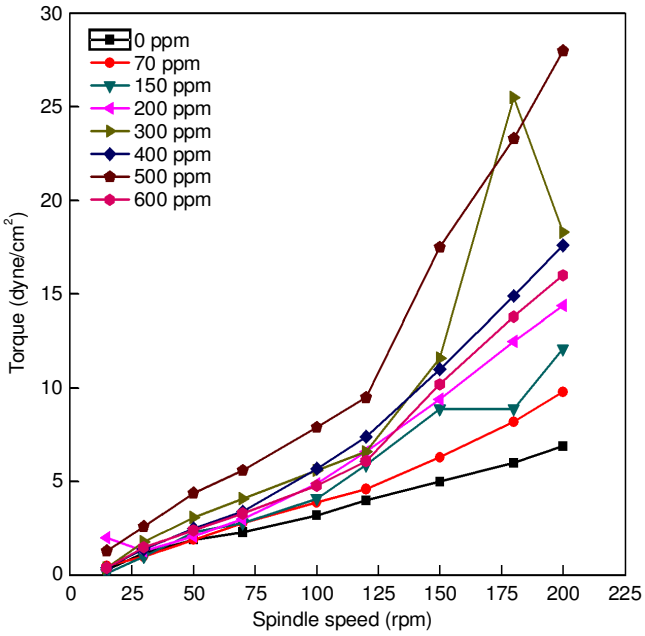

Fig. 3. Torque *vs.* spindle speed variation for polyacrylamide solution

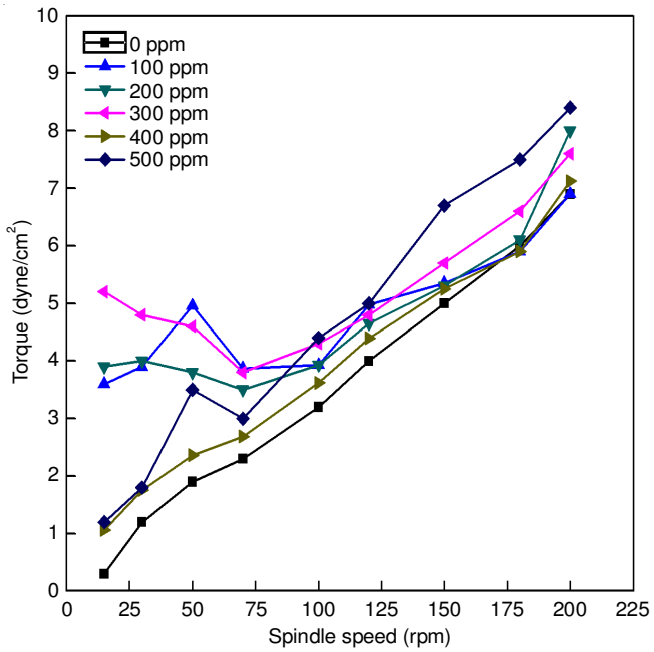

Fig. 4. Torque *vs.* spindle speed variation for polyethylene oxide solution

typically range from 2 to 30 dyne/cm^2. For polyethylene oxide (Fig. 4), the addition of the polymer also causes an increase in applied torque for different rpm readings when compared to water (0 ppm) solution. The range of torque values range from 0.2 to 9 dyne/cm^2 with maximum torque reached for 500 ppm solution. The 400 ppm polyethylene oxide solution shows the closest proximity to pure water. The experimental data collected here is compared with the results from Akindoyo *et al.* [4] where Xanthan gum is added to water and essentially the same setup is used to monitor torque variation with rotational speed. Fig. 5 compares the results for 70 ppm solution of polyacrylamide, 100 ppm polyethylene oxide and 150 ppm Xanthan gum. The general trend observed in this study is consistent with that reported in literature and shows an almost linear

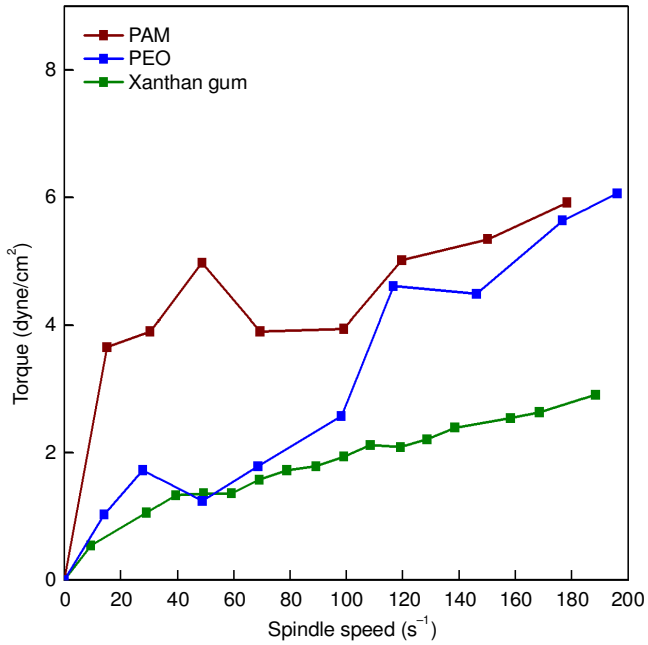

Fig. 5. Comparison of torque *vs.* spindle speed for polyacrylamide and polyethylene oxide solutions with Xanthan gum solution [Ref. 4]

increase in torque with rotational speed of the spindle. Also, the slope seems to have a direct correlation with the molecular weight of the added species. Higher molecular weight polyacrylamide shows greatest slope followed by polyethylene oxide and Xanthan gum [4]. The literature quotes the molecular weight of the gum used as 2×10^6 g/mol. The difference in torque ranges for polyacrylamide and polyethylene oxide solutions differ greatly with that for polyacrylamide solution in the range from 2 to 30 dyne/cm^2 and for polyethylene oxide solution in the range from 0.2 to 9 dyne/cm^2.The difference can be attributed to the fact that the chosen polyacrylamide (20×10^6 g/mol) sample is of higher molecular weight than polyethylene oxide (6×10^6 g/mol). Thus polyacrylamide particles contribute to the higher resistive nature of the subject fluid requiring the higher torque.

Variation of torque against strain rate: The torque (or stress) *versus* strain rate curve depicted in Fig. 6 shows the typical kinds of fluids we encounter in fluid dynamics. A comparative analysis for torque with strain rate is done here for sample fluid solutions used in this study in order to infer their fluid flow characteristics.

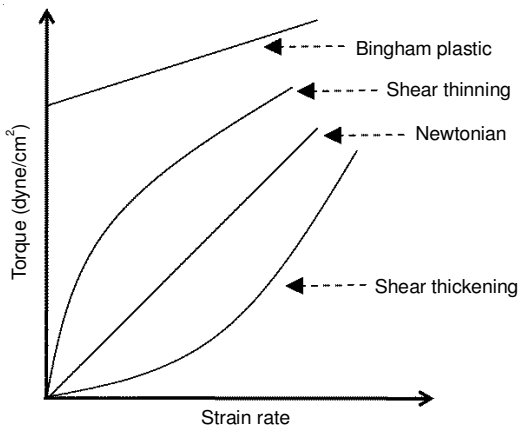

Fig. 6. Typical torque *versus* strain rate curves for different types of fluids

Figs. 7 and 8 show that the addition of polyacrylamide and polyethylene oxide brings about a deviation from the Newtonian characteristics of water. The extent of deviation is lesser in case of polyethylene oxide compared to polyacrylamide. This can be accounted from the fact that maximum torque reached for same shear strain values is about 9 dyne/cm^2 whereas for polyacrylamide solutions the maximum torque reached is about 18 dyne/cm^2. Inference can be drawn from Figs. 7 and 8 that introduction of the polymer into water brings about a drastic change in the characteristics of fluid. A significant change in fluid flow properties can be observed as the polyacrylamide solutions bring about steadier flows with significant increase in the shear viscosity of the fluid. This

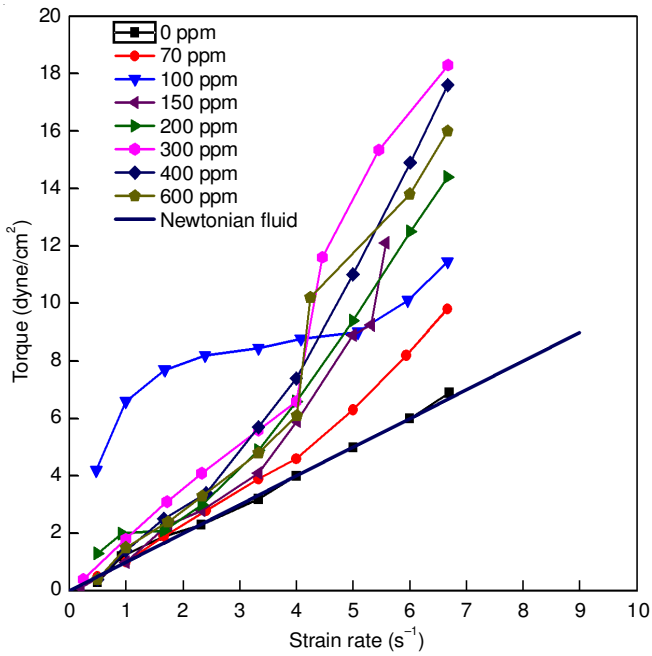

Fig. 7. Torque *vs.* strain rate curve for polyacrylamide solution

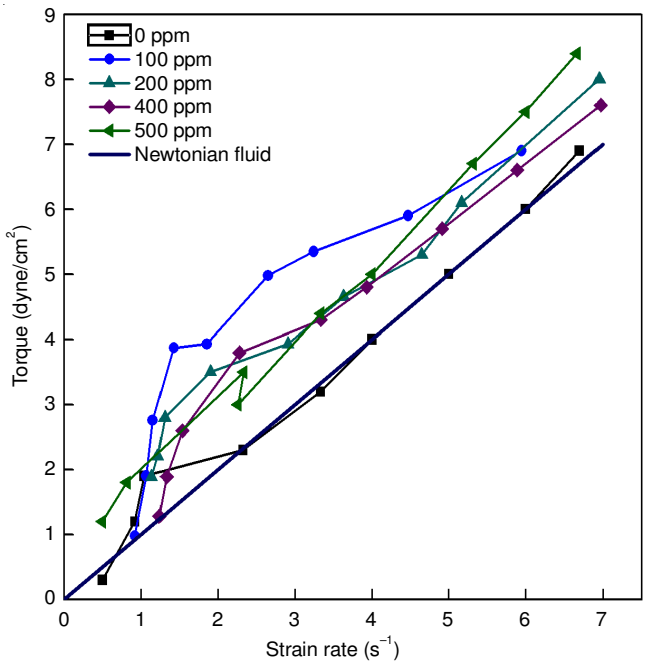

Fig. 8. Torque *vs.* strain rate curve for polyethylene oxide solution

can clearly account for relatively larger departure of polyacrylamide solutions from Newtonian fluid curve when compared to the polyethylene oxide solutions. The observations are in coherence with the results obtained in literature [9].

Variation of viscosity against rotational speed: The plot of viscosity *versus* rotational speed for polyacrylamide solutions shows increase in viscosity values with rotational speeds (Fig. 9). This is due to the reason that the greater torque delivery is needed by the spindle to attain the same rotational speeds and lower strain rates. This tendency is observed more in higher ppm polymer solutions. For instance, 300 ppm and 400 ppm polyacrylamide solutions show an increase in viscosity by a factor of as much as 2.3. The data for polyethylene oxide (Fig. 10) reveals that at lower rotational speeds, polyethylene oxide solutions show greater resistance to strain (torque applied) hence it has greater viscosity. As the rpm value is increased the viscosity goes down. For 70 and 100 ppm solutions, a reduction of as much as a factor of one-third of its initial values is noted. This can be related to the greater strain rates achieved for increasing stress (torque) with the rotational speed. Such tendency is significantly lower for higher ppm solutions. Both solutions have an opposite response for viscosity with increase in rotational speed. The increase in rpm brings about a small rise in viscosity for all polyacrylamide solutions whereas for polyethylene oxide there is a consistent decrease in viscosity with increase in rpm. The observed behaviour can be attributed to the higher molecular weight and the ionic nature of the polyacrylamide solution which has larger molecules posing greater internal resistance to flow as the torque increases. This is relatively lower in polyethylene oxide since they do not carry displaced charges within their structure and have fairly lower size when compared to polyacrylamide. With the help from the Figs. 9 and 10, polymer-water solutions can be narrowed down to the ones that show the closest viscous behaviour to water and at the same time suppress turbulent viscosity by exhibiting viscoelastic nature as shown in Figs. 7 and 8. A

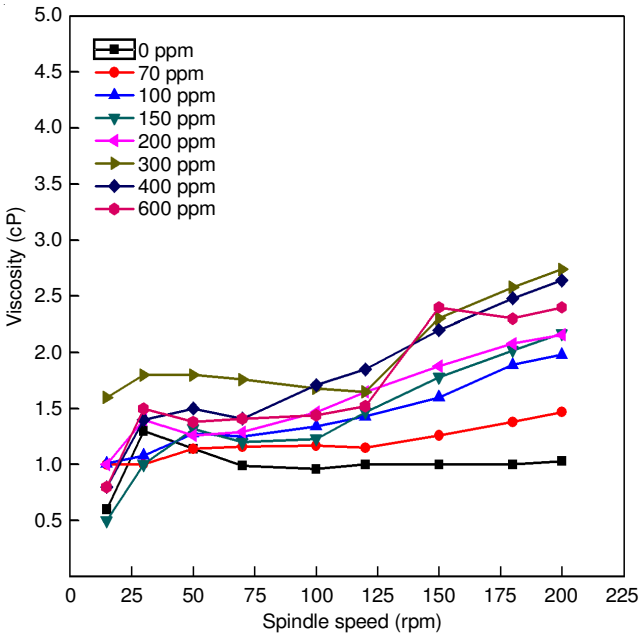

Fig. 9. Viscosity *vs*. spindle speed for polyacrylamide solution

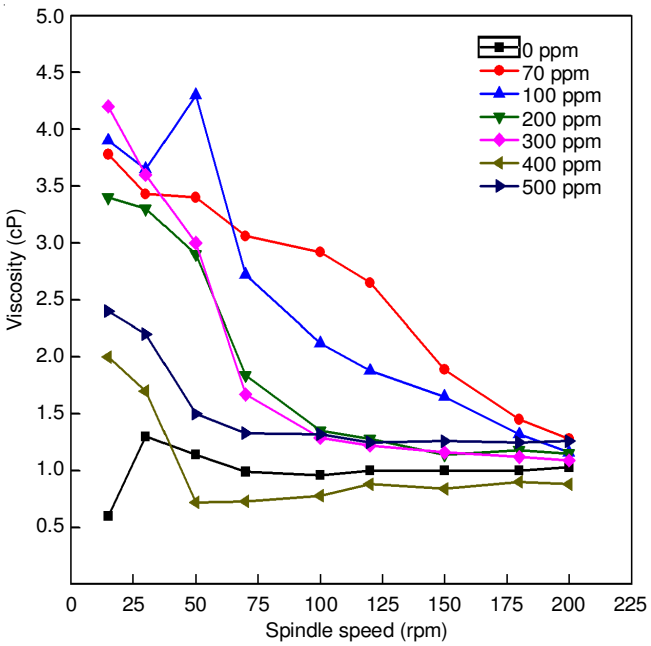

Fig. 10. Viscosity *vs*. spindle speed for polyethylene oxide solution

comparative analysis of the plots suggests that 70 ppm solution of polyacrylamide and 400 ppm solution of polyethylene oxide show the best drag reducing characteristics in the range of experimental conditions investigated in this work.

Conclusion

The present study reports an experimental investigation of the viscoelastic nature of drag reducing polymers (polyacrylamide and polyethylene oxide) added aqueous solutions using intensive viscometry. Concentration ranges from 0 to 600 ppm of polymer additives in water are studied in order to compare their drag reducing characteristics. Putting these findings into perspective, it is concluded that this particular technology can be applied in numerous fields where fluid transportation is required. Future work should aim at utilizing these properties in spray equipment, sewage water treatment systems, crude oil transport through pipes and boat hull or submarine designs. Besides this, field irrigation and transportation of sludge and slurries are other areas of potential applications. At the same time, further research should be done to find out viable natural long chain bio polymers as substitute for the synthetic ones.

ACKNOWLEDGEMENTS

The authors gratefully acknowledge to SRM University for providing the laboratory facilities throughout the course of this research project.

REFERENCES

1. P.K. Ptasinski, F.T.M. Nieuwstadt, B.H.A.A. van den Brule and M.A. Hulsen, *Flow Turbul. Combus.*, **66**, 159 (2001); https://doi.org/10.1023/A:1017985826227.
2. T. Min, J. Yul Yoo, H. Choi and D.D. Joseph, *J. Fluid Mech.*, **486**, 213 (2003); https://doi.org/10.1017/S0022112003004610.
3. A.H. Barnes, A Handbook of Elementary Rheology, University of Wales, Institute of Non-Newtonian Fluid Mechanics: Aberystwyth, edn 1 (2000).

4. E.O. Akindoyo, H.A. Abdulbari and Z. Yousif, *Int. J. Res. Eng. Technol.*, **4**, 84 (2015).
5. D. Kulmatova, Ph.D. thesis, Turbulent Drag Reduction by Additives, Van der Waals-Zeeman Institute (WZI), Amsterdam, Netherlands (2013).
6. C.V. Subbarao, D.A. Naidu and P. King, *Int. J. Appl. Sci. Eng.*, **11**, 159 (2013).
7. H.P. Soni and D.P. Bharambe, *Iran. Polym. J.*, **15**, 943 (2006).
8. F. Holland and R. Bragg, Fluid Flow for Chemical and Process Engineers, Elsevier: Burlington, edn 1 (1995).
9. J.M.J. Den Toonder, M.A. Hulsen, G.D.C. Kuiken and F.T.M. Nieuwstadt, *J. Fluid Mech.*, **337**, 193 (1997); https://doi.org/10.1017/S0022112097004850.
10. M.D. Graham, *Rheol. Rev.*, **2**, 143 (2004).
11. G. Nesyn, K. Konovalov, O. Vetrova and P. Menshov, *Procedia Chem.*, **15**, 371 (2015); https://doi.org/10.1016/j.proche.2015.10.059.
12. A.A. Khadom and A.A. Abdul-Hadi, *Ain Shams Eng. J.*, **5**, 861 (2014); https://doi.org/10.1016/j.asej.2014.04.005.
13. C.M. White and M.G. Mungal, *Annu. Rev. Fluid Mech.*, **40**, 235 (2008); https://doi.org/10.1146/annurev.fluid.40.111406.102156.
14. A. Japper-Jaafar, M.P. Escudier and R.J. Poole, *J. Non-Newt. Fluid Mech.*, **161**, 86 (2009); https://doi.org/10.1016/j.jnnfm.2009.04.008.
15. G.M.H. Nieuwenhuys, Masters Thesis, Effect of Drag-Reducing Polymers on a Vertical Multiphase Flow, Delft University of Technology, Delft, Netherlands (2003).
16. M.H. Hassanean, M.E. Awad, H. Marwan, A.A. Bhran and M. Kaoud, *Egypt. J. Petrol.*, **25**, 39 (2016); https://doi.org/10.1016/j.ejpe.2015.02.013.
17. B. Yu, F. Li and Y. Kawaguchi, *Int. J. Heat Fluid Flow*, **25**, 961 (2004); https://doi.org/10.1016/j.ijheatfluidflow.2004.02.029.
18. A.S. Pereira, R.M. Andrade and E.J. Soares, *J. Non-Newt. Fluid Mech.*, **202**, 72 (2013); https://doi.org/10.1016/j.jnnfm.2013.09.008.
19. A.A. Mohsenipour, R. Pal and K. Prajapati, *Can. J. Chem. Eng.*, **91**, 181 (2013); https://doi.org/10.1002/cjce.20686.